Power-Law Scaling of Synchronization Robustly Reproduced in the Hippocampal CA3 Slice Culture Model with Small-World Topology

Toshikazu Samura[1], Yasuomi D. Sato[2,3], Yuji Ikegaya[4], Hatsuo Hayashi[2], and Takeshi Aihara[1]

[1] Tamagawa University Brain Science Institute,
6-1-1 Tamagawa Gakuen, Machida, Tokyo 194-8610, Japan
{samura,aihara}@eng.tamagawa.ac.jp
[2] Graduate School of Life Science and Systems Engineering,
Kyushu Institute of Technology,
2-4 Hibikino, Wakamatsu-ku, Kitakyushu 808-0196, Japan
{sato-y,hayashi}@brain.kyutech.ac.jp
[3] Frankfurt Institute for Advanced Studies (FIAS),
Johann Wolfgang Goethe University,
Ruth-Moufang-Str. 1, Frankfurt am Main, 60438, Germany
sato@fias.uni-frankfurt.de
[4] Laboratory of Chemical Pharmacology,
Graduate School of Pharmaceutical Sciences,
The University of Tokyo, Tokyo 113-0033, Japan
ikegaya@mol.f.u-tokyo.ac.jp

Abstract. The hippocampal CA3 is a recurrent network included small-world topology. The percentage of co-active neurons in CA3 slice cultures is approximated by power-law. We show that the power-law scaling of synchronization is reproduced in the CA3 slice culture model where synaptic weights are log-normally distributed and balanced excitation/inhibition regardless of network topologies. However, small-world topology improves the robustness of the reproduction of the power-law scaling in the culture model. Power-law scaling is known as a sign of optimization of a network for information processing. These results suggest that CA3 may be robustly optimized for information processing by excitation/inhibition balance, log-normally distributed synaptic weights and small-world topology.

Keywords: Hippocampal CA3, Synchronization, Power-law scaling, Log-normal distribution, Excitation/inhibition balance, Small-world topology.

1 Introduction

The hippocampus consists of dentate gyrus (DG), CA3 and CA1. The hippocampal CA3 region is anatomically unique in the hippocampus. Pyramidal

T. Huang et al. (Eds.): ICONIP 2012, Part II, LNCS 7664, pp. 152–159, 2012.
© Springer-Verlag Berlin Heidelberg 2012

neurons in CA3 are mutually connected with other CA3 neurons [1]. Takahashi *et al.* have found the small-world topology of CA3 network from synchronized spontaneous activity in CA3 slice cultures [2]. Therefore, the hippocampal CA3 network is considered as a recurrent network with small-world topology. They have also revealed power-law scaling in the spontaneous activity. Synchrony size that is the percentage of neurons emitting a spike in 10 ms time bin is approximated by power-law. Synchronized neuronal activity obeyed power-law is called as a neuronal avalanche [3]. Neuronal avalanches have been observed in many brain regions. It has been suggested that information capacity, information transmission and dynamic range are maximized in the cortical network with neuronal avalanches [4] [5]. These mean that CA3 network where power-law scaling emerges may be optimized for the hippocampal information processing.

In this study, we reproduce the power-law scaling of synchronization in CA3 slice cultures by using a CA3 slice culture model. The slice model consists of excitatory and inhibitory neurons described by the Izhikevich neuron model [6]. Each neuron in the model is connected with other neurons to become the small-world network. We show that the high reproducibility of the power-law scaling emerges in the slice model when the synaptic weights are log-normally distributed and inhibition balances with excitation. Additionally, we change the network topology from regular to random. Although the power-law scaling is reproduced in the network regardless of network topologies, small-world topology improves the robustness of the reproduction of the power-law scaling. The frequency of the high reproductivity becomes high in the small-world network. In other words, the power-law scaling is robustly reproduced in the small-world network. These results suggest that CA3 may be optimized for information processing by excitation/inhibition balance and log-normally distributed synaptic weights, and then the small-world topology enhances the robustness of the optimization.

2 Materials and Methods

2.1 Power-Law Scaling of Synchronization in CA3 Slice Culture

The activities of neurons in CA3 slice cultures obtained by high-speed functional multineuron calcium imaging (fMCI) at 32 degrees Celsius are available at http://hippocampus.jp/data/. We used the activities of $1,193$ neurons in 14 slices. The sampling rate is 500 Hz and recording time is 130 sec. Each slice includes 53–137 neurons, but pyramidal cells and interneurons are not identified in the data. Figure 1 shows the cumulative distribution of synchrony size. Synchrony size is the percentage of neurons emitting spike in 10 ms time bin. As referred to [7], we calculated cumulative distribution $C_{\exp}(s)$ of synchrony size from experimental data. The probability of synchrony size obeys a power-law distribution [2]. The distribution of synchrony size exhibited the linearity on a log-log scale (Fig.1).

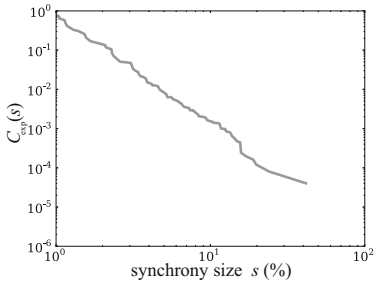

Fig. 1. The cumulative distribution of synchrony size calculated from the experimental data

2.2 Reproducibility of the Power-Law Scaling

We defined distance between the cumulative distributions of synchrony size obtained from experimental data ($C_{\mathrm{exp}}(s)$) and simulation results ($C_{\mathrm{sim}}(s)$) as the reproducibility of the power-law activity. We calculated an overlapped range between $C_{\mathrm{exp}}(s)$ and $C_{\mathrm{sim}}(s)$. Ten points are selected from the overlapped range. The points are evenly spaced on the logarithmic scale. The distance (i.e. reproducibility) r is given by

$$r = \frac{1}{10}\sum_{i=1}^{10} \mid \log(\frac{C_{\mathrm{exp}}^{\mathrm{est}}(s_i)}{C_{\mathrm{sim}}^{\mathrm{est}}(s_i)}) \mid, \tag{1}$$

where $C^{\mathrm{est}}(s_i)$ is the estimated cumulative distribution at the ith point s_i by kernel density estimation. When r approaches zero, the degree of reproducibility becomes high.

2.3 CA3 Slice Culture Model

We constructed a CA3 slice model that is a recurrent network consisting of excitatory and inhibitory neurons. Both neurons are modeled by using the Izhikevich model [6]. The Izhikevich model is given by

$$v_i' = 0.04v_i^2 + 5v_i + 140 - u_i - I_i(t), \tag{2}$$
$$u_i' = a(bv_i - u_i), \tag{3}$$

where i is neuron index. v_i is the membrane potential and u_i is the membrane recovery variable. a is the rate of recovery. b is the sensitivity of the recovery variable. $I_i(t)$ is the inputs from other neurons to the ith neuron and calculated by the following equation:

$$I_i(t) = g_i^{\mathrm{ex}}(v_i - V_{\mathrm{ex}}) + g_i^{\mathrm{inh}}(v_i - V_{\mathrm{inh}}) + g_i^{\mathrm{noise}}(v_i - V_{\mathrm{noise}}),$$

where V_{ex}, V_{inh} and V_{noise} are the reversal potential for excitatory, inhibitory and noise inputs. We set these parameters as follows: $V_{\mathrm{ex}} = V_{\mathrm{noise}} = 0$ mV, $V_{\mathrm{inh}} = -75$ mV. g_i^{ex}, g_i^{inh} and g_i^{noise} are conductance for each input given by

$$g_i^{x'} = -g_i^x/\tau_{\mathrm{in}} + \sum_j^{N_i^x} w_{ij} \sum_k^{N_j^{\mathrm{fired}}} \delta(t - t_j^k - \tau_{ij}), \tag{4}$$

$$g_i^{\mathrm{noise}'} = -g_i^{\mathrm{noise}}/\tau_{\mathrm{in}} + w_{\mathrm{noise}}\delta(t - t_{\mathrm{noise}}^k), \tag{5}$$

where $x \in \{\mathrm{ex}, \mathrm{inh}\}$, τ_{in} (=8.0 [ms]) is a time constant for each input. N_i^{ex} (N_i^{inh}) is the total number of presynaptic excitatory neurons (inhibitory interneurons) of the ith neuron. w_{ij} means the synaptic weight between the ith and jth neurons. N_j^{fired} is the number of firing of the jth presynaptic neuron. $\delta(\cdot)$ is the Dirac delta function and t_j^k is the kth firing timing of the jth neuron. τ_{ij} (=1.0 [ms]) is the synaptic delay between the ith and jth neurons. $w_{\mathrm{noise}}(= 1.0)$ is the strength of a noise input and the t^k is kth noise timing of the jth neuron. Let the ith neuron fire a spike when v_i arrives at 30 mV and v_i and are u_i reset as follows:

$$\text{if } v_i \geq 30, \text{ then } \begin{cases} v_i \leftarrow c \\ u_i \leftarrow u_i + d. \end{cases} \tag{6}$$

Then v_i and u_i are abruptly reset to c and $u_i + d$, respectively. An excitatory neuron and an inhibitory neuron were modeled by regular spiking neuron [6], so that we set parameters as follows: $a = 0.02, b = 0.2, c = -65, d = 8$.

We assumed that each neuron is driven by noise inputs and fires at respective frequency. To assigned unique firing frequency to each neuron, we randomly selected value from an exponential distribution ($\lambda = 0.25$) as a base frequency parameter f_i of the ith neuron. When the f_i is over 0.2, we selected f_i from the exponential distribution again to avoid excess firing frequency. The intervals of noise input timing (t_{noise}^k) of the ith neuron obeyed a exponential distribution ($\lambda = 1.0/f_i$ sec.).

The number of excitatory neurons (N_{ex}) in a CA3 slice is 50–140 randomly selected. Since we assume that the ratio of pyramidal cell to inhibitory interneuron is 10 : 1 in the hippocampus, as referred to [1], the number of interneurons (N_{inh}) was 10 % of excitatory neurons. Excitatory neurons arranged on ring lattice points (Fig. 2 (a)). Interneurons were distributed uniformly to keep the distances between inhibitory interneurons on the ring. An excitatory neuron connected to the nearest 9 % neurons of excitatory neurons (E−E), and all inhibitory interneurons within a range where there are connected excitatory neurons (E−I). The connection probability from inhibitory interneurons to excitatory neurons is 60 %. The connections were rewired to randomly selected neurons with probability $p = 0.05$, but inhibitory interneurons were rewired only to excitatory pyramidal cells. There were no inhibitory connections among inhibitory interneurons (Fig. 2 (a)). Additionally, the number of each type of connections (E−E, E−I, and I−E) is kept before and after rewiring. By increasing the rewiring probability p, the network among excitatory neurons changes

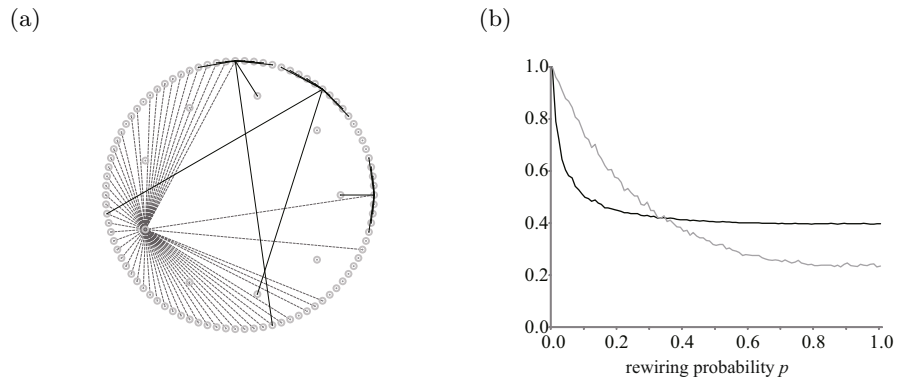

Fig. 2. Structure of CA3 slice culture model. (a) Arrangement and connections of each neuron. As a matter of convenience, although both the types of neurons are arranged on the same ring, excitatory neurons and inhibitory neurons are plotted as gray dots on outside and inside circle, respectively. A part of connections is shown by lines. Each excitatory neuron connects with other nearest excitatory neurons and inhibitory interneurons (black lines). Each inhibitory interneuron connects only with other nearest excitatory neurons (gray dashed lines). However, a part of their connections is rewired to distant neurons. (b) Clustering coefficient (gray line) and average path length (black line) in the network among excitatory neurons rewired at each probability. Each value is normalized by the value obtained at $p = 0$.

from regular to random network. The clustering coefficient is high and average path length is low around the rewiring probability $p = 0.05$; therefore the network topology is the small-world [8](Fig. 2 (b)).

We defined synaptic weights of each type of connections. It has been reported that the distribution of synaptic strength in the visual cortex layer 5 can be fitted by a log-normal distribution [9]. The distribution has a heavier tail and strong connections probably exist in the network. Therefore, we set the synaptic weight of a connection as randomly selected value from a log-normal distribution because the distribution of synaptic weight in CA3 is still unknown. The strengths of E−E connections were randomly selected value from a log-normal distribution ($\mu = \log(0.17) + \sigma^2$, $\sigma = \log(2.0)$). The strengths of E−I and I−E connections were randomly selected value from a log-normal distribution ($\mu = \log(W_{\{\mathrm{EI\ or\ IE}\}}) + \sigma^2$, $\sigma = \log(2.0)$). We changed W_{EI} and W_{IE} from 0.1 to 0.4 in 0.01 steps, respectively.

3 Results

Using the CA3 slice model, we obtained the activities of all neurons from 10 trials on each combination of W_{EI} and W_{IE}. In each trial, we recorded the activities of neurons for 130 sec in 150 sec to exclude initial 20 sec. The cumulative distribution of synchrony size was obtained from neuronal activities in 10 trials.

We calculated the distance between the cumulative distributions of synchrony size obtained from the experimental data and simulation results on each combination (Fig. 3(a)).

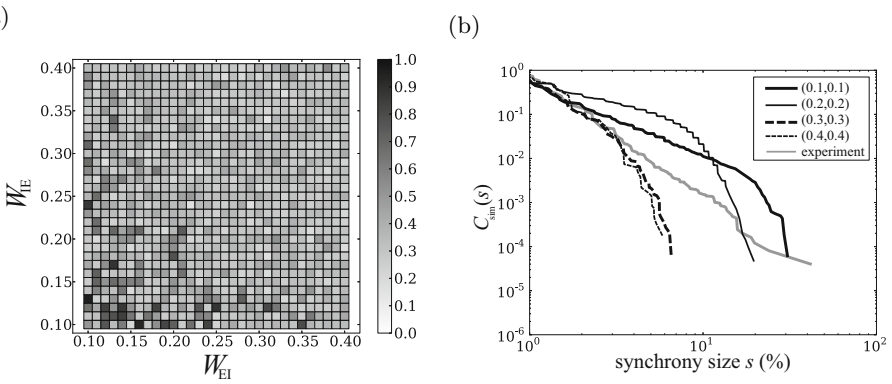

Fig. 3. Reproduction of the power-law scaling in the CA3 slice model. (a) Distance between experimental data and simulation results on each combination of W_{EI} and W_{IE}. (b) The cumulative density of synchrony size obtained on each of four combinations along the diagonal line from bottom-left to top-right in Fig. 3(a) ($W_{\mathrm{EI}} = W_{\mathrm{IE}} = \{0.1, 0.2, 0.3, 0.4\}$).

Inhibitory interneurons are driven by not only noise input, but also inputs through E−I connections. Therefore, the change of synaptic weight (W_{EI} and W_{IE}) corresponds to the change of the strength of inhibition. The inhibition is weakest on the bottom-left corner, while the inhibition is strongest on the top-right corner. Since the distance changed from long to short along the diagonal line from bottom-left to top-right, the reproducibility of power-law was affected by the strength of inhibition. Figure 3 (b) shows the cumulative distribution of synchrony size at each of four points on the diagonal line ($W_{\mathrm{EI}} = W_{\mathrm{IE}} = \{0.1, 0.2, 0.3, 0.4\}$). When inhibition was weak ($W_{\mathrm{EI}} = W_{\mathrm{IE}} = \{0.1, 0.2\}$), excess synchronization tends to occur compared to the experiments. On the other hand, when inhibition was strong ($W_{\mathrm{EI}} = W_{\mathrm{IE}} = \{0.3, 0.4\}$), excess synchronization tends not to occur. It was expected that properly strong inhibition causes the power-law distributed activity in the network. Indeed, as shown in Fig. 4 (b), similar power-law scaling emerges in the network when $W_{\mathrm{EI}} = 0.31$ and $W_{\mathrm{IE}} = 0.34$. The small-world network with log-normally distributed synaptic weights and inhibition balance with excitation reproduces the power-law scaling.

We changed rewiring probability p from 0.05 (small-world) to 0.0 (regular network) or 1.0 (random network). The power-law scaling similar to the experimental data emerged regardless of the network topology (Fig. 4 (a-c)). Fig. 4 (d) shows the cumulative distribution of distance obtained from each network topology on all combination of W_{EI} and W_{IE}. The distribution obtained from the small-world topology shows a steep slope. This result indicates that the distance frequently becomes small in the small-world network on the combinations

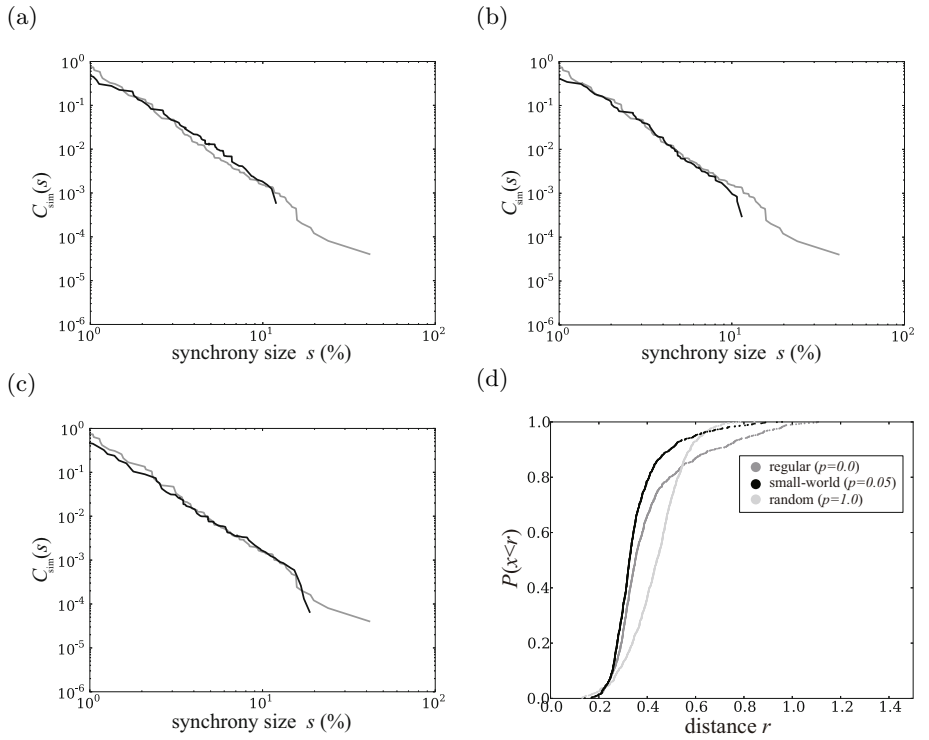

Fig. 4. Cumulative distribution of synchrony size (a–c) and distance obtained (d) in each network topology. (a–c) Cumulative distribution of synchrony size when the distance becomes minimum in each network topology: (a) regular ($p = 0.0$, $W_{\mathrm{EI}} = 0.37$ and $W_{\mathrm{IE}} = 0.31$), (b) small-world ($p = 0.05$, $W_{\mathrm{EI}} = 0.31$ and $W_{\mathrm{IE}} = 0.34$) and (c) random network ($p = 1.0$, $W_{\mathrm{EI}} = 0.37$ and $W_{\mathrm{IE}} = 0.14$). (d) Cumulative distribution of distance in each network topology.

compared to other topologies. In other words, the high reproducibility robustly emerges in the small-word network.

4 Conclusion and Discussion

We have found that the high reproducibility of the power-law scaling emerges in the slice model regardless of the rewiring probability when the synaptic weights are log-normally distributed and inhibition balances with excitation. These results consist with the experimental results that power-law scaling disappears on cortical slice culture with imbalance between excitation and inhibition [5]. The distribution of synaptic weights in CA3 have not been reported yet; however log-normally distributed synaptic weights are observed from the visual cortex [9]. Our results suggest that the log-normally distributed synaptic weights may

be observed from the hippocampal CA3 in experiments. On the other hand, small-world topology in the slice model frequently reproduced power-law scaling of synchronization. When power-law scaling emerges in a network, the network is optimized for information processing [4] [5]. Small-world recurrent network with excitation/inhibition balance and log-normally distributed synaptic weights robustly cause power-law scaling; therefore CA3 may be robustly optimized for information processing.

Acknowledgements. T.S. and T.A. were supported by MEXT -Supported Program for the Strategic Research Foundation at Private Universities, 2009–2013. Y.I. was supported by the Funding Program for Next Generation World-Leading Researchers (no. LS023).

References

1. Traub, R.D., Miles, R.: Neuronal Networks of the Hippocampus. Cambridge Univ. Press, New York (1991)
2. Takahashi, N., Sasaki, T., Matsumoto, W., Matsuki, N., Ikegaya, Y.: Circuit Topology for Synchronizing Neurons in Spontaneously Active Networks. Proc. Natl. Acad. Sci. USA 107, 10244–10249 (2010)
3. Beggs, J.M., Plenz, D.: Neuronal avalanches in neocortical circuits. J. Neurosci. 23, 11167–11177 (2003)
4. Shew, W.L., Yang, H., Petermann, T., Roy, R., Plenz, D.: Neuronal avalanches imply maximum dynamic range in cortical networks at criticality. J. Neurosci. 29, 15595–15600 (2009)
5. Shew, W.L., Yang, H., Yu, S., Roy, R., Plenz, D.: Information capacity and transmission are maximized in balanced cortical networks with neuronal avalanches. J. Neurosci. 31, 55–63 (2011)
6. Izhikevich, E.M.: Simple Model of Spiking Neurons. IEEE Trans. Neural Netw. 14, 1569–1572 (2003)
7. Klaus, A., Yu, S., Plenz, D.: Statistical analyses support power law distributions found in neuronal avalanches. PloS One 6, e19779 (2011)
8. Watts, D.J., Strogatz, S.H.: Collective dynamics of 'small-world' networks. Nature 393, 440–442 (1998)
9. Song, S., Sjostrom, P.J., Reigl, M., Nelson, S., Chklovskii, D.B.: Highly nonrandom features of synaptic connectivity in local cortical circuits. PLoS Biol. 3, e68 (2005)